

Origin of the tiny energy gap and Dirac points in monoclinic trilayer nickelate $\text{La}_4\text{Ni}_3\text{O}_{10}$

Hu Zhang

*Hebei Research Center of the Basic Discipline for Computational Physics, Hebei Key
Laboratory of High-precision Computation and Application of Quantum Field Theory,
College of Physics Science and Technology, Hebei University, Baoding 071002,
People's Republic of China*

E-mails: zhanghu@hbu.edu.cn

Superconductivity was recently found in trilayer nickelate $\text{La}_4\text{Ni}_3\text{O}_{10}$ under high pressure with a phase transition from the monoclinic $P2_1/a$ structure to the tetragonal $I4/mmm$ structure. Previous experimental works have confirmed the existence of a tiny energy gap formed with Ni $3d_{z^2}$ orbitals in monoclinic $\text{La}_4\text{Ni}_3\text{O}_{10}$. Here we investigate the physical origin of this gap by analyzing symmetry properties of energy bands based on the group theory. The tiny gap comes from energy bands with opposite parity at the Brillouin zone center. In addition, we also find previously unknown Dirac points in some momentum directions around the Fermi level. An effective Hamiltonian is constructed to describe low energy physics of the tiny energy gap and Dirac points. Due to the low crystal symmetry of monoclinic $\text{La}_4\text{Ni}_3\text{O}_{10}$, its energy bands display strong anisotropic properties.

I. INTRODUCTION

Since the discovery of superconductivity in $\text{Nd}_{0.8}\text{Sr}_{0.2}\text{NiO}_2$ thin film in 2019 [1], layered nickelate oxides have attracted more and more attention. Recently, superconductivity near 80 K was found in Ruddlesden-Popper nickelate $\text{La}_3\text{Ni}_2\text{O}_7$ under high pressure [2]. There existed a structure transition from the orthorhombic (*Amam*) structure to the orthorhombic (*I4/mmm*) structure when $\text{La}_3\text{Ni}_2\text{O}_7$ is compressed [3]. Similar to $\text{La}_3\text{Ni}_2\text{O}_7$, superconductivity was also found very recently in trilayer nickelate $\text{La}_4\text{Ni}_3\text{O}_{10}$ under high pressure [4,5]. A phase transition from the monoclinic $P2_1/a$ (or $P2_1/c$ with a different choice of axis) to the tetragonal *I4/mmm* structure was confirmed. The electronic structure difference between different crystal structures in phase transitions is important to understand the mechanism of superconductivity in nickelates. For both $\text{La}_3\text{Ni}_2\text{O}_7$ and $\text{La}_4\text{Ni}_3\text{O}_{10}$, the Ni $3d_{z^2}$ orbital is believed to play a critical role for the appearance of superconductivity [2].

For $\text{La}_4\text{Ni}_3\text{O}_{10}$ with the monoclinic $P2_1/a$ space group, a 20 meV energy gap near the Fermi level was found by angle-resolved photoemission spectroscopy (ARPES) measurements and theoretical band structure calculations [6,7]. This energy gap is formed by the band of principally Ni $3d_{z^2}$ orbital, which is very important to understand physical properties of monoclinic $\text{La}_4\text{Ni}_3\text{O}_{10}$. However, the origin of such energy gap is not well investigated up to now. To fully understand electronic structures of $\text{La}_4\text{Ni}_3\text{O}_{10}$, we should find out the physical origin of this tiny energy gap.

In this work, we firstly analyze the symmetry of electronic energy bands of monoclinic $\text{La}_4\text{Ni}_3\text{O}_{10}$ with the $P2_1/a$ space group detailly with the help of group theory. Then, the origin of the energy gap is discussed. A low energy effective model is constructed to describe the low energy physics of energy gap based on the theory of invariant. In addition, through careful analysis of energy bands in the entire Brillouin zone, we also discover previously unrecognized Dirac points formed by Ni $3d_{z^2}$ orbital contributed bands near the Fermi level in some momentum directions.

II. METHODOLOGY

We have performed first-principles calculations based on density functional theory

(DFT) [8] with the Perdew–Burke–Ernzerhoff (PBE) functional in generalized gradient approximation (GGA) [9] in the Vienna Ab Initio Simulation Package (VASP) [10-12]. We used a $12 \times 12 \times 12$ Monkhorst-Pack grid [13] and an energy cutoff of 500 eV. The $k \cdot p$ method was used to obtain the effective Hamiltonian.

III. RESULTS AND DISCUSSION

A. Symmetry properties of monoclinic $\text{La}_4\text{Ni}_3\text{O}_{10}$

The space group number of monoclinic $\text{La}_4\text{Ni}_3\text{O}_{10}$ is 14. Due to the different choice of axis, the space group is denoted as $P2_1/a$ or $P2_1/c$. Recent experiments [4,14] for monoclinic $\text{La}_4\text{Ni}_3\text{O}_{10}$ with space group $P2_1/a$ at ambient pressure give $a = 5.4164 \text{ \AA}$, $b = 5.4675 \text{ \AA}$, $c = 14.2279 \text{ \AA}$, $\alpha = \beta = 90^\circ$, and $\gamma = 100.752^\circ$. For the notation of $P2_1/c$, $a = 14.2279 \text{ \AA}$, $b = 5.4675 \text{ \AA}$, $c = 5.4164 \text{ \AA}$, $\alpha = \gamma = 90^\circ$, and $\beta = 100.752^\circ$. To simplify the analysis of energy bands, we use the setting of $P2_1/c$ space group in this work. Different choices do not change the physics. In Fig. 1(a) we show atomic structures of primitive cell of monoclinic $\text{La}_4\text{Ni}_3\text{O}_{10}$ with the $P2_1/c$ space group. There are two formulas containing six Ni atoms in the primitive cell. As a result of strong distortions of NiO_6 , this phase has very low symmetry.

The corresponding Brillouin zone of the primitive cell of monoclinic $\text{La}_4\text{Ni}_3\text{O}_{10}$ with the $P2_1/c$ space group is plotted in Fig. 1(b) in which high symmetry points are denoted. To better understand the energy band, we should firstly know the little point group of various high symmetry points. The little point groups of points Γ (0, 0, 0), Z (0, 0.5, 0), B (0, 0, 0.5), and D (0, 0.5, 0.5) located in the $k_x = 0$ plane are all C_{2h} (2/m). The point in the B-D direction is denoted as point V (0, u, 0.5) with symmetry of C_2 (2). The point group for Λ (0, u, 0) located at the Γ -Z direction is also C_2 . Both Y (0.5, 0, 0) and A_0 (0.5, 0, 0) have symmetry C_{2h} . There is also an important point F (v, 0, u) in the $k_y = 0$ plane with the point group C_s (m). The point located at the Γ -D direction is a general point (GP) with symmetry C_1 (1). These results are collected in Table I.

The point group C_{2h} has four group elements: identity E , a two-fold rotation c_{2y}

around the y axis, inversion I and a mirror $\sigma_h = Ic_{2y}$. Two group generators of the point group C_{2h} are c_{2y} and I with matrix forms:

$$\begin{aligned} R(c_{2y}) &= \begin{pmatrix} -1 & 0 & 0 \\ 0 & 1 & 0 \\ 0 & 0 & -1 \end{pmatrix}, \\ R(I) &= \begin{pmatrix} -1 & 0 & 0 \\ 0 & -1 & 0 \\ 0 & 0 & -1 \end{pmatrix}. \end{aligned} \quad (1)$$

Each element of the point group C_{2h} forms a class. Hence C_{2h} contains four classes. As a result, there are four one-dimensional irreducible representations Γ_1^+ , Γ_1^- , Γ_2^+ and Γ_2^- . The character table of point group C_{2h} is given in Table II.

From knowledge of group theory, we know that C_2 , C_s and C_1 are all subgroups of C_{2h} . Both C_2 and C_s have two group elements. C_2 contains two group elements: identity E and c_{2y} . Two group elements for C_s are E and a mirror σ_h . For both C_2 and C_s , each element forms a class. Thus, each of them has two one-dimensional irreducible representations Γ_1 and Γ_2 . The point group C_1 only contains one element E and thus only has one one-dimensional irreducible representation Γ_1 . According to these symmetry properties and Brillouin zone shown in Fig. 1(b), we may expect that electronic energy bands in the $k_y = 0$ and $k_x = 0$ planes might be very different. All these symmetry information will help us to understand electronic energy bands of monoclinic $\text{La}_4\text{Ni}_3\text{O}_{10}$.

B. The energy gap in monoclinic $\text{La}_4\text{Ni}_3\text{O}_{10}$

Now we analysis the origin of the tiny energy gap in monoclinic $\text{La}_4\text{Ni}_3\text{O}_{10}$ discovered in previous works. In Fig. 2 we plot electronic energy bands of monoclinic $\text{La}_4\text{Ni}_3\text{O}_{10}$ (primitive cell) with the $P2_1/c$ space group along high-symmetry directions of the Brillouin zone calculated with the above noted experimental lattice parameters. Our results are identical to previous experimental and theoretical works [6,7]. Energy bands are projected to Ni $3d_{x^2-y^2}$ (red) and Ni $3d_{z^2}$ (blue) orbitals. There is a tiny energy gap around the Brillouin zone center Γ point near the fermi level E_F , which is formed by energy bands with the Ni $3d_{z^2}$ orbital character. This tiny energy gap has been confirmed experimentally [6] and is the important prominent feature of

monoclinic $\text{La}_4\text{Ni}_3\text{O}_{10}$.

As noted above, the point group of the Brillouin zone center Γ point is C_{2h} with four irreducible representations $\Gamma_{1,2}^{+,-}$. Based on symmetry analysis, we find that energy bands forming the gap at the Γ point transform according to the Γ_2^+ and Γ_2^- irreducible representations of C_{2h} , as shown in Fig. 2. From above section we also know that, the momentum k point located at the Γ -Z direction is denoted as Λ with symmetry C_2 having irreducible representations Γ_1 and Γ_2 (denoted as Λ_1 and Λ_2 now) and the point located at the Γ -D direction is GP with symmetry C_1 having an irreducible representation Γ_1 (denoted as GP_1 now). Compatibility relations in the group theory give the symmetry of energy bands at nearby k points. According to compatibility relations between Γ and Z (GP), both Γ_2^+ and Γ_2^- bands at the Γ point become Λ_2 bands at the Λ point or GP_1 bands at the GP point. These results are also displayed in Fig. 2. Since energy bands with the same symmetry character cannot cross, there are always energy gaps at Λ and GP points. This is usually called the anti-crossing in condensed matter physics. Thus, the tiny energy gap in monoclinic $\text{La}_4\text{Ni}_3\text{O}_{10}$ origins from energy bands having symmetry Γ_2^+ and Γ_2^- with opposite parity at the Brillouin zone center Γ point. Only from these symmetry properties of energy bands near the Fermi level E_F can we get a better understanding of the tiny energy gap.

We now construct a low energy effective Hamiltonian to describe the tiny energy gap around the Brillouin zone center Γ point in monoclinic $\text{La}_4\text{Ni}_3\text{O}_{10}$. We need two generators c_{2y} and I of the point group C_{2h} . From knowledge of characters of the point group C_{2h} given in Table II, the symmetry representations in Γ_2^+ and Γ_2^- bands are given by

$$\begin{aligned} D(c_{2y}) &= \begin{pmatrix} -1 & 0 \\ 0 & -1 \end{pmatrix}, \\ D(I) &= \begin{pmatrix} 1 & 0 \\ 0 & -1 \end{pmatrix}. \end{aligned} \quad (2)$$

The theory of invariant gives the following constraint on $k \cdot p$ model [15]

$$D(R)H(k)D^\dagger(R) = H(R(k)), \quad (3)$$

where $D(R)$ is the representative matrix of operator R . Based on these we obtain the $k \cdot p$ effective Hamiltonian (to second order in k) describing the tiny energy gap formed by Γ_2^+ and Γ_2^- bands around the Fermi level E_F in monoclinic $\text{La}_4\text{Ni}_3\text{O}_{10}$

$$H(k) = \varepsilon(k) + \begin{pmatrix} M(k) & (\alpha_3 - i\alpha_4)k_y \\ (\alpha_3 + i\alpha_4)k_y & -M(k) \end{pmatrix}, \quad (4)$$

with $\varepsilon(k) = \alpha_1 + \alpha_5 k_x^2 + \alpha_7 k_y^2 + \alpha_9 k_z^2 + \alpha_{11} k_x k_z$, $M(k) = \alpha_2 + \alpha_6 k_x^2 + \alpha_8 k_y^2 + \alpha_{10} k_z^2 + \alpha_{12} k_x k_z$ and $\alpha_i (= 1 \sim 12)$ are materials dependent parameters. We have eigenenergies:

$$E(k) = \varepsilon(k) \pm \sqrt{(\alpha_3^2 + \alpha_4^2)k_y^2 + M(k)^2}. \quad (5)$$

These energy bands show strong anisotropy in $k_{x,y,z}$ directions, which comes from low crystal symmetry of monoclinic $\text{La}_4\text{Ni}_3\text{O}_{10}$ shown in Fig. 1(a). The off-diagonal k_y term in the Hamiltonian results from the group generator two-fold rotation c_{2y} of point group C_{2h} reflecting its different properties from k_x and k_z directions. The tiny energy gap is related to terms in the square root in (5). With this Hamiltonian we can have more accurate understanding of energy bands formed with Ni $3d_{z^2}$ orbitals. In the next section, we will investigate the anisotropic properties of energy bands in monoclinic $\text{La}_4\text{Ni}_3\text{O}_{10}$.

C. Dirac points

From above two discussions we know that monoclinic $\text{La}_4\text{Ni}_3\text{O}_{10}$ has strong anisotropic symmetry properties. To having complete knowledge of energy bands in the entire Brillouin zone, in Fig. 3(a) we plot the two-dimensional energy bands at the $k_x = 0$ plane (Z- Γ -B-D) contributed by the Ni $3d_{z^2}$ orbital near the Fermi level E_F around the Γ point. The energy gap can be found clearly. Amazingly, there are crossing points in k points located at the Γ -B (k_z) direction. Energy bands around the crossing point are shown in Fig. 3(b). In Fig. 4(a) we plot the electronic energy bands along high-symmetry B- Γ -A₀ directions of the Brillouin zone. As discussed above, k points in the $k_y = 0$ plane are denoted as F ($v, 0, u$) with symmetry C_s having two one-dimensional irreducible representations F_1 and F_2 . Hence points between Γ and B (A₀) are all F. From compatibility relations, Γ_2^+ and Γ_2^- bands at the Γ point become

F_2 and F_1 bands, respectively, at the F point. According to knowledge of group theory, energy bands with different symmetry characters are allowed to cross. As a result, F_2 and F_1 bands cross at the F point as can be found in Fig. 4(a). Such crossing point is called the Dirac point like that in graphene [16,17]. Therefore, except the tiny energy gap, Ni $3d_{z^2}$ orbitals in monoclinic $\text{La}_4\text{Ni}_3\text{O}_{10}$ also form Dirac points. The energy bands in Γ -Z (k_y) and Γ -B (k_z) directions have very different properties, which comes from their different symmetry properties as Λ and F points having point groups C_2 and C_s respectively. The Dirac point is protected by the mirror symmetry σ_h in C_s . There is a linear energy-momentum relation around Dirac points as can be found in Fig. 3(b).

To see electronic energy bands in the k_x direction (Γ -Y), in Fig. 4(b) we plot electronic energy bands along high-symmetry B- Γ -Y directions of the Brillouin zone shown with symmetry characters. The k point in the Γ -Y direction is also F ($v, 0, u$), in which energy bands having F_2 and F_1 symmetry. Different from energy bands in the Γ -B direction, F_2 and F_1 bands do not crossing along the Γ -Y direction. In Fig. 5 we plot two-dimensional energy bands at the $k_y = 0$ plane (Y- Γ -B- A_0) contributed by the Ni $3d_{z^2}$ orbital near the Fermi level E_F around the Γ point. The up band is very flat near Γ . While the down band looks like the surface of a saddle. Anisotropic band crossing characters between two bands can be found clearly. These results demonstrate that energy bands of monoclinic $\text{La}_4\text{Ni}_3\text{O}_{10}$ have strong anisotropy. Such character origins from anisotropy of its atomic structures. As can be found in Fig. 1(a), the distorted Ni-O planes tilt along the crystal lattice a . This leads that energy bands in k_x and k_z shown in Fig. 4(a) and 4(b) have very different dispersions. The strong distortions of NiO_6 results in very low crystal symmetry.

Previous experiments mainly focus on energy bands in the Z- Γ -D direction and thus do not find the Dirac points. In future ARPES experiments, Dirac points can be observed directly by focusing on energy bands in the B- Γ - A_0 direction. Both the tiny energy gap and Dirac points are important electronic characters of monoclinic $\text{La}_4\text{Ni}_3\text{O}_{10}$. These results also indicate the special role of the Ni $3d_{z^2}$ orbital.

Different physical properties of energy bands along k_x , k_y and k_z directions in

monoclinic $\text{La}_4\text{Ni}_3\text{O}_{10}$ can also be understood from our Hamiltonian in (5). If $k_y = 0$, the off-diagonal term in Hamiltonian $H(k)$ disappears and thus $H(k)$ is a diagonal matrix. For $k_x = k_z = 0$, we have:

$$E(k_y) = \alpha_1 + \alpha_7 k_y^2 \pm \sqrt{(\alpha_3^2 + \alpha_4^2)k_y^2 + (\alpha_2 + \alpha_8 k_y^2)^2}. \quad (6)$$

While for $k_x = k_y = 0$, we have:

$$E(k_z) = \alpha_1 + \alpha_9 k_z^2 \pm (\alpha_2 + \alpha_{10} k_z^2). \quad (7)$$

These show very different energy-momentum relations. Hence energy bands in k_y (Γ -Z) and k_z (Γ -B) with very different crossing properties are expected. This is consistent with the appearance of tiny energy gap and Dirac point in Fig. 2 and Fig. 4(a) respectively. Low crystal symmetry of monoclinic $\text{La}_4\text{Ni}_3\text{O}_{10}$ makes its energy bands having anisotropic properties. In a word, symmetry determines different dispersing electronic excitations in momentum space.

IV. CONCLUSIONS

In summary, we have investigated electronic structures of monoclinic $\text{La}_4\text{Ni}_3\text{O}_{10}$ detailly. Based on group theory, we find that the tiny energy gap observed in previous experimental works origins from energy bands with opposite parity at the Brillouin zone center. In addition, previously unknown Dirac points in other momentum directions are also discovered. Energy bands of monoclinic $\text{La}_4\text{Ni}_3\text{O}_{10}$ have strong anisotropy due to its low crystal symmetry. Our works help to understand electronic characters of monoclinic $\text{La}_4\text{Ni}_3\text{O}_{10}$.

ACKNOWLEDGMENTS

This work was supported by the Advanced Talents Incubation Program of the Hebei University (Grants No. 521000981423, No. 521000981394, No. 521000981395, and No. 521000981390), the Natural Science Foundation of Hebei Province of China (Grants No. A2021201001 and No. A2021201008), the National Natural Science Foundation of China (Grants No. 12104124 and No. 12274111), the Central Guidance on Local Science and Technology Development Fund Project of Hebei Province

(236Z0601G), Scientific Research and Innovation Team of Hebei University (No. IT2023B03), and the high-performance computing center of Hebei University.

TABLE I. The little point groups for high symmetry k points in Brillouin zone of primitive cell of monoclinic $\text{La}_4\text{Ni}_3\text{O}_{10}$ with space group $P2_1/c$.

k point	Little group	k point	Little group
Γ (0, 0, 0)	C_{2h} (2/m)	Λ (0, u, 0)	C_2 (2)
Z (0, 0.5, 0)	C_{2h} (2/m)	Y (0.5, 0, 0)	C_{2h} (2/m)
B (0, 0, 0.5)	C_{2h} (2/m)	A_0 (0.5, 0, 0)	C_{2h} (2/m)
D (0, 0.5, 0.5)	C_{2h} (2/m)	F (v, 0, u)	C_s (m)
V (0, u, 0.5)	C_2 (2)		

TABLE II. Table of characters for point group C_{2h} (2/m).

	E	C_{2y}	I	σ_h
Γ_1^+ (A_g)	1	1	1	1
Γ_1^- (A_u)	1	1	-1	-1
Γ_2^+ (B_g)	1	-1	1	-1
Γ_2^- (B_u)	1	-1	-1	1

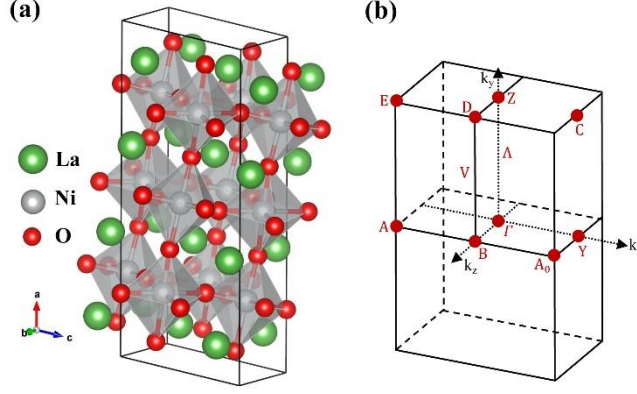


FIG. 1. (a) Atomic structures of monoclinic $\text{La}_4\text{Ni}_3\text{O}_{10}$ with the space group $P2_1/c$. (b) The Brillouin zone of the primitive cell of monoclinic $\text{La}_4\text{Ni}_3\text{O}_{10}$ shown with high symmetry points.

The F point is located at $(v, 0, u)$.

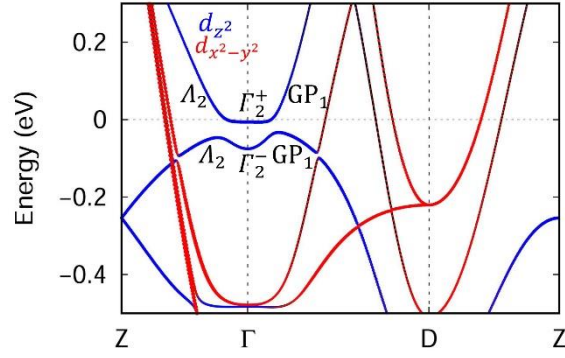


FIG. 2. First-principles calculated electronic band dispersions of monoclinic $\text{La}_4\text{Ni}_3\text{O}_{10}$ with the space group $P2_1/c$. The points between Γ and Z (D) are denoted as Λ (GP). The color lines indicate the projection to the Ni $3d_{x^2-y^2}$ (red) and Ni $3d_{z^2}$ (blue) states. Symmetry characters of energy bands are also shown.

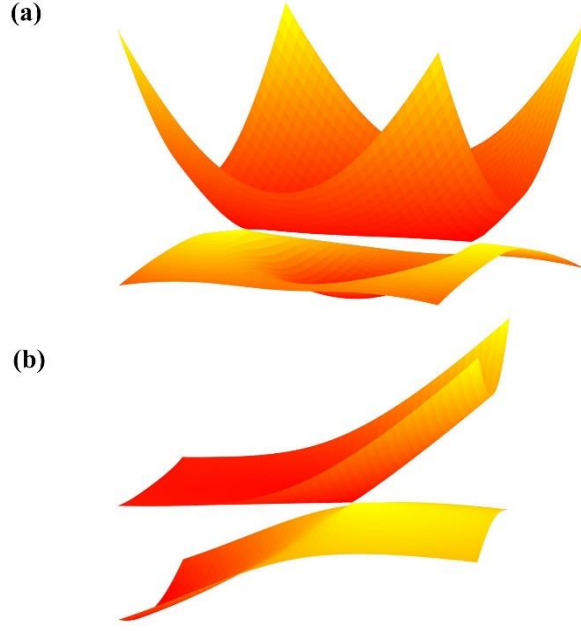


FIG. 3. (a) Two-dimensional energy bands of monoclinic $\text{La}_4\text{Ni}_3\text{O}_{10}$ at the $k_x = 0$ plane contributed by the Ni $3d_{z^2}$ orbital near the Fermi level E_F around the Γ point. (b) Two-dimensional energy bands around the crossing point (Dirac point).

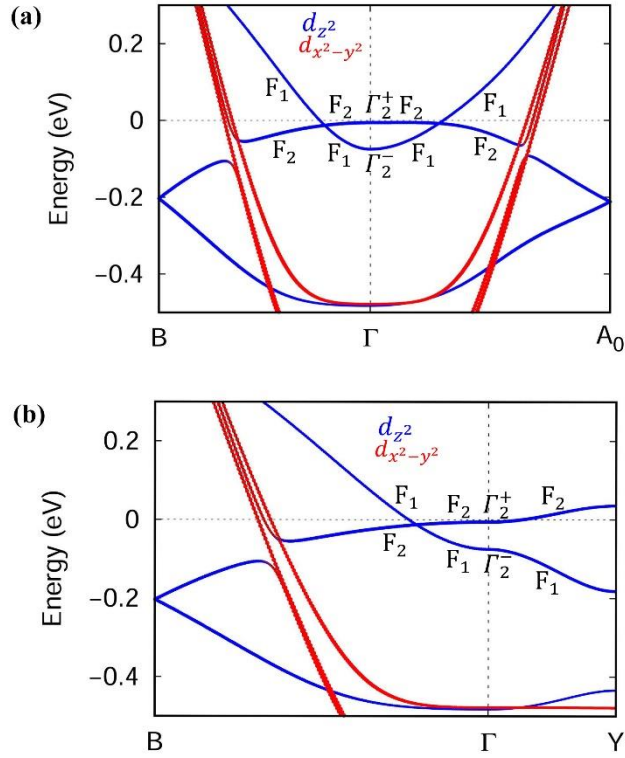


FIG. 4. First-principles calculated electronic band dispersions of monoclinic $\text{La}_4\text{Ni}_3\text{O}_{10}$ along high-symmetry (a) B- Γ - A_0 and (b) B- Γ -Y directions with the F ($v, 0, u$) point denoted. The color

lines indicate the projection to the Ni $3d_{x^2-y^2}$ (red) and Ni $3d_{z^2}$ (blue) states. Symmetry characters of energy bands are also shown.

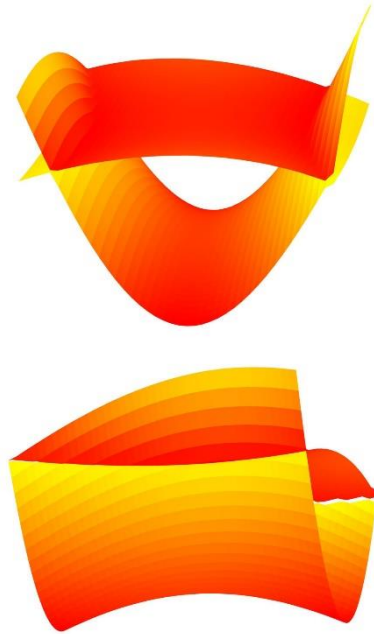


FIG. 5. Two-dimensional energy bands of monoclinic $\text{La}_4\text{Ni}_3\text{O}_{10}$ at the $k_y = 0$ plane contributed by the Ni $3d_{z^2}$ orbital near the Fermi level E_F around the Γ point.

- [1] D. Li, K. Lee, B. Y. Wang, M. Osada, S. Crossley, H. R. Lee, Y. Cui, Y. Hikita, and H. Y. Hwang, Superconductivity in an infinite-layer nickelate, *Nature* **572**, 624 (2019).
- [2] H. Sun *et al.*, Signatures of superconductivity near 80 K in a nickelate under high pressure, *Nature* **621**, 493 (2023).
- [3] L. Wang *et al.*, Structure responsible for the superconducting state in La₃Ni₂O₇ at low temperature and high pressure conditions, arXiv:2311.09186.
- [4] M. Zhang *et al.*, Superconductivity in trilayer nickelate La₄Ni₃O₁₀ under pressure, arXiv:2311.07423.
- [5] Y. Zhu *et al.*, Superconductivity in pressurized trilayer La₄Ni₃O₁₀- δ single crystals, *Nature* **631**, 531 (2024).
- [6] H. Li, X. Zhou, T. Nummy, J. Zhang, V. Pardo, W. E. Pickett, J. F. Mitchell, and D. S. Dessau, Fermiology and electron dynamics of trilayer nickelate La₄Ni₃O₁₀, *Nat. Commun.* **8**, 704 (2017).
- [7] D. Puggioni and J. M. Rondinelli, Crystal structure stability and electronic properties of the layered nickelate La₄Ni₃O₁₀, *Phys. Rev. B* **97** (2018).
- [8] R. O. Jones, Density functional theory: Its origins, rise to prominence, and future, *Rev. Mod. Phys.* **87**, 897 (2015).
- [9] J. P. Perdew, K. Burke, and M. Ernzerhof, Generalized Gradient Approximation Made Simple, *Phys. Rev. Lett.* **77**, 3865 (1996).
- [10] G. Kresse and J. Furthmüller, Efficient iterative schemes for ab initio total-energy calculations using a plane-wave basis set, *Phys. Rev. B* **54**, 11169 (1996).
- [11] M. Gajdoš, K. Hummer, G. Kresse, J. Furthmüller, and F. Bechstedt, Linear optical properties in the projector-augmented wave methodology, *Phys. Rev. B* **73** (2006).
- [12] J. Hafner, Ab-initio simulations of materials using VASP: Density-functional theory and beyond, *J Comput Chem* **29**, 2044 (2008).
- [13] H. J. Monkhorst and J. D. Pack, Special points for Brillouin-zone integrations, *Phys. Rev. B* **13**, 5188 (1976).
- [14] Y. Zhu *et al.*, Signatures of superconductivity in trilayer La₄Ni₃O₁₀ single crystals, arXiv:2311.07353.
- [15] D. Gresch, Q. Wu, G. W. Winkler, and A. A. Soluyanov, Hidden Weyl points in centrosymmetric paramagnetic metals, *New J. Phys.* **19**, 035001 (2017).
- [16] N. P. Armitage, E. J. Mele, and A. Vishwanath, Weyl and Dirac semimetals in three-dimensional solids, *Rev. Mod. Phys.* **90**, 015001 (2018).
- [17] A. H. Castro Neto, F. Guinea, N. M. R. Peres, K. S. Novoselov, and A. K. Geim, The electronic properties of graphene, *Rev. Mod. Phys.* **81**, 109 (2009).